**Supplementary Information**

# Sodium-Ion Diffusion and Voltage Trends in Phosphates $Na_4M_3(PO4)_2P_2O_7$ (M= Fe, Mn, Co, Ni) for Possible High Rate Cathodes

Stephen M. Wood[a], Chris Eames[a], Emma Kendrick[b,c] and M. Saiful Islam[a*]

[a] Department of Chemistry, University of Bath, Claverton Down, Bath BA2 7AY, UK

[b] SHARP Laboratories of Europe Limited, Oxford OX4 4GB, UK

[c] School of Chemistry, University of Birmingham, Edgbaston, Birmingham B15 2TT, UK

**Table S1:** Potential model developed, for use in MD simulations, based on potentials of Pedone et al. O-O, P-O and Na-O potentials were unchanged over those from the Pedone model.[1]

| Interaction | D (eV) | α ($Å^{-2}$) | r (Å) | C | Y |
|---|---|---|---|---|---|
| Fe-O | 0.066171 | 1.772638 | 2.658163 | 2.0 | 1.2 |
| Mn-O | 0.032616 | 2.0255701 | 2.719217 | 3.0 | 1.2 |

**Table S2:** Deviation (Δ) between calculated and experimental structures[2,3] of $Na_4M_3(PO_4)_2P_2O_7$ from Pedone potential model used in MD calculations.

| Lattice Parameter | Fe | | Mn | |
|---|---|---|---|---|
| | Expt | Calc | Expt | Calc |
| a/Å | 18.07517 | 18.47168 | 17.991 | 18.486 |
| b/Å | 6.53238 | 6.60949 | 6.648 | 6.630 |
| c/Å | 10.64760 | 10.89843 | 10.765 | 10.992 |
| α/° | 90.0 | 90.0 | 90.0 | 90.0 |
| β/° | 90.0 | 90.0 | 90.0 | 90.0 |
| γ/° | 90.0 | 90.0 | 90.0 | 90.0 |

**Table S3:** $U_{eff}$ values used in various DFT+U computational studies of Li-ion and Na-ion battery materials.

| Transition Metal | Material Class | U-J Value (eV) | Reference |
|---|---|---|---|
| $Mn^{2+}/Mn^{3+}$ | Borate | 3.9 | Ceder et al.[4] |
| | Carbonophosphate | 3.9 | Ceder et al.[5] |
| | Sulphate | 3.9 | Islam et al.[6] |
| | Oxide and phosphate | 4.0 | Ceder et al.[7] |
| | Silicate | 4.0 | Dompablo et al.[8] |
| | Silicate | 4.0 | Dompablo et al.[9] |
| | Borate | 4.5 | Kang et al.[10] |
| | Fluorophosphate | 4.5 | Kang et al.[11] |
| | Phosphate | 4.5 | Kang et al.[12] |
| | Oxide Spinel | 5.0 | Kang et al.[13] |
| $Mn^{3+}/Mn^{4+}$ | Oxide | 3.9 | Kang et al.[14] |
| | Oxide | 4.0 | Meng et al.[15] |
| | Oxide | 5.0 | Meng et al.[16] |
| | Oxide | 5.0 | Meng et al.[17] |
| | Oxide | 5.0 | Dompablo et al.[18] |
| | Oxide Spinel | 5.0 | Meng et al.[19] |
| | Oxide | 5.1 | Islam et al.[20] |
| | Oxide | 5.2 | Islam et al.[21] |
| $Fe^{2+}/Fe^{3+}$ | Oxide and phosphate | 3.9 | Ceder et al.[7] |
| | Silicate | 4.0 | Kang et al.[22] |
| | Carbonophosphate | 4.0 | Ceder et al.[5] |
| | Hydroxysulfate | 4.0 | Islam et al.[23] |
| | Silicate | 4.0 | Islam et al.[24] |
| | Silicate | 4.0 | Dompablo et al.[25] |

| | | | |
|---|---|---|---|
| | Silicate | 4.0 | Dompablo et al.[26] |
| | Sulphate | 4.0 | Islam et al.[6] |
| | Silicate | 4.0 | Dompablo et al.[9] |
| | Borate | 4.3 | Kang et al.[10] |
| | Mixed Phosphate | 4.3 | Kang et al.[2] |
| | Phosphate | 4.3 | Kang et al[12] |
| | Phosphate | 4.3 | Ceder et al.[27] |
| | Oxide Spinel | 5.0 | Kang et al.[13] |
| $Fe^{3+}/Fe^{4+}$ | Oxide | 4.0 | Ceder et al.[28] |
| $Ni^{2+}/Ni^{3+}$ | Silicate | 4.0 | Dompablo et al.[9] |
| | Carbonophosphate | 6.0 | Ceder et al.[5] |
| $Ni^{3+}/Ni^{4+}$ | Oxide | 5.96 | Meng et al.[16] |
| | Oxide | 5.96 | Meng et al.[17] |
| | Oxide | 5.96 | Dompablo et al.[18] |
| | Oxide Spinel | 5.96 | Meng et al.[19] |
| | Oxide | 6.1 | Meng et al.[15] |
| | Oxide | 6.0 | Ceder et al.[28] |
| $Co^{2+}/Co^{3+}$ | Oxide Spinel | 4.3 | Kang et al.[13] |
| | Silicate | 4.0 | Dompablo et al.[8] |
| | Silicate | 4.0 | Dompablo et al.[9] |
| | Borate | 5.7 | Kang et al.[10] |
| | Carbonophosphate | 5.7 | Ceder et al.[5] |
| | Phosphate | 5.7 | Kang et al.[12] |
| | Sulphate | 5.7 | Islam et al.[6] |
| $Co^{3+}/Co^{4+}$ | Oxide | 3.0 | Meng et al.[29] |
| | Oxide | 3.4 | Ceder at el.[28] |

**Table S4:** Potential model developed, for use in defect energy calculations, covering the class of materials $Na_4M_3(PO_4)_2P_2O_7$[M = Fe, Mn, Ni and Co] .

| Interaction | A | ρ | C | k | Y |
|---|---|---|---|---|---|
| Na-O | 2612.0 | 0.2644 | 0.0 | 9999 | 1.0 |
| P-O | 1194.0 | 0.3385 | 0.0 | 9999 | 5.0 |
| O-O | 22764.3 | 0.149 | 44.53 | 65.0 | 0.96 |
| Fe-O | 1450.0 | 0.2977 | 0.0 | 19.16 | -0.997 |
| Mn-O | 1068.8 | 0.3154 | 0.0 | 81.2 | -1.0 |
| Ni-O | 1900.08 | 0.280 | 0.0 | 2.88 | 0.0 |
| Co-O | 3245.0 | 0.2644 | 0.0 | 110.5 | -1.503 |

**Table S5:** Published data on $Na^+$ ion diffusion coefficients for sodium-ion cathode materials.

| Diffusion Coefficients Range | Material | Reference |
|---|---|---|
| $10^{-14}$ | Na rich layered oxides | Zhou et al.[30] |
| $10^{-16}$ - $10^{-12}$ | $Na_{0.44}MnO_2$ | Kim et al.[31] |
| $10^{-14}$ - $10^{-13}$ | $Na_{0.44}MnO_2$ | Kim et al.[32] |
| $10^{-8}$ | $MnO_2$ | Tseng et al.[33] |
| $10^{-11}$ | $Na_xCoO_2$ | Moritomo et al.[34] |
| $10^{-11}$ | $Na_xMnO_2$ | Moritomo et al.[35] |
| $10^{-8}$ - $10^{-7}$ | $Na_xCoO_2$ | Chou et al.[36] |
| $10^{-15}$ - $10^{-13}$ | $NaMn_3O_5$ | Zhou et al.[37] |
| $10^{-14}$ | $Na_2V_6O_{16}.H_2O$ | Shang et al.[38] |
| $10^{-15}$ - $10^{-13}$ | $Na_3V_2(PO_4)_3$ | Balducci et al.[39] |
| $10^{-10}$ | $Na_3V_2(PO_4)_2F$-$_3C$ | Wei et al.[40] |
| $10^{-12}$ | $Na_3V_2(PO_4)F$ | Banks et al.[41] |
| $10^{-14}$ - $10^{-12}$ | $V_2O_5$ | Kohl et al.[42] |

| | | |
|---|---|---|
| $10^{-15}$ | $NaFePO_4$ | Mentus et al.[43] |
| $10^{-10}$ | $Na_{0.66}[Li_{0.22}Ti_{0.78}]O_2$ | Huang et al.[44] |
| $10^{-11}$ | $Li_4Ti_5O_{12}$ | Yang et al.[45] |

**Table S6:** Structural reproduction of $Na_4M_3(PO_4)_2P_2O_7$ from DFT simulations, for M = Fe, Mn and Ni, compared to experimental data.[2,3]

| Lattice Parameter | Fe | | Mn | | Ni | |
|---|---|---|---|---|---|---|
| | Expt | Calc | Expt | Calc | Expt | Calc |
| a/Å | 18.07517 | 18.11671 | 17.991 | 18.056 | 17.999 | 18.035 |
| b/Å | 6.53238 | 6.53176 | 6.648 | 6.651 | 6.4986 | 6.4681 |
| c/Å | 10.64760 | 10.64427 | 10.765 | 10.781 | 10.4200 | 10.3609 |

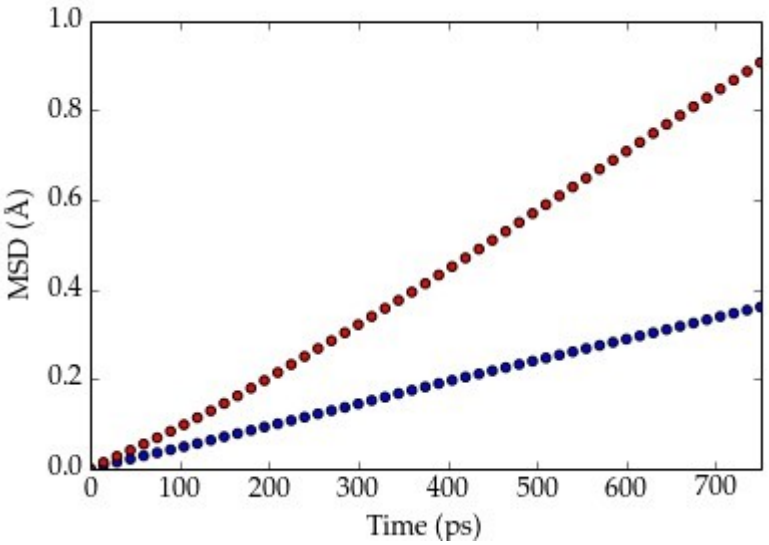


**Figure S1:** Mean square displacement (MSD) plots for Na-ion diffusion in $Na_{3.8}M_3(PO_4)_2P_2O_7$ for M=Fe (blue) and M=Mn (red) at 625 K.

**Intrinsic defects**

Kroger Vink notation detailing the defects explored in atomistic simulations. The equations refer to Na Frenkel, M Frenkel (M = Fe, Mn, Ni and Co), P Frenkel, O Frenkel, Schottky and antisite defects respectively.

$$Na_{Na}^{\times} \rightarrow V_{Na}' + Na_i^{\bullet}$$

$$M_M^{\times} \rightarrow V_M'' + M_i^{\bullet\bullet}$$

$$P_P^{\times} \rightarrow V_P'''' + P_i^{\bullet\bullet\bullet\bullet\bullet}$$

$$O_O^{\times} \rightarrow V_O^{\bullet\bullet} + O_i''$$

$$4\,Na_{Na}^{\times} + 3\,M_M^{\times} + 4\,P_P^{\times} + 15\,O_O^{\times} \rightarrow V_{Na}' + V_M'' + V_P'''' + V_O^{\bullet\bullet} + Na_4M_3(PO_4)_2P_2O_7$$

$$Na_{Na}^{\times} + M_M^{\times} \rightarrow Na_M' + M_{Na}^{\bullet}$$

**Thermodynamic Stability**

We explored the feasibility of doping by calculating the formation enthalpy of solid solutions and hence performing a convex-hull analysis, displayed in figure S2. It is found that for the Mn material (figure 5 (a)) the $Na_4Fe_2Mn(PO_4)_2P_2O_7$ phase lies above the convex hull and as such is predicted to phase separate into the $Na_4FeMn_2(PO_4)_2P_2O_7$ and $Na_4Fe_3(PO_4)_2P_2O_7$ compositions under low temperature equilibration conditions. The convex hull for the Ni doped material is shown in figure S2 (b) and demonstrates significantly different behaviour to that of the Mn doped material. All compositions of the sodiated phase lie along the convex hull; however the formation enthalpies are low, (~1-10 meV per formula unit), and as such the doped phases are likely to be unstable at room temperature. In addition, the desodiated phases demonstrate a miscibility gap across the composition range. As such in the bulk we predict that these doped phases are unstable and thus solid solutions are unlikely to be synthesized, instead separating into the $Na_4Fe_3(PO_4)_2P_2O_7$ and $Na_4Ni_3(PO_4)_2P_2O_7$ phases. We note that most

materials are synthesised at high temperatures. It is possible that with the high temperature formation this would help, but the materials would need to be quenched for the solid solution to remain. In any case, since the $Na_4Fe_2Ni(PO_4)_2P_2O_7$ material is predicted to display an attractive voltage, this warrants further investigation.

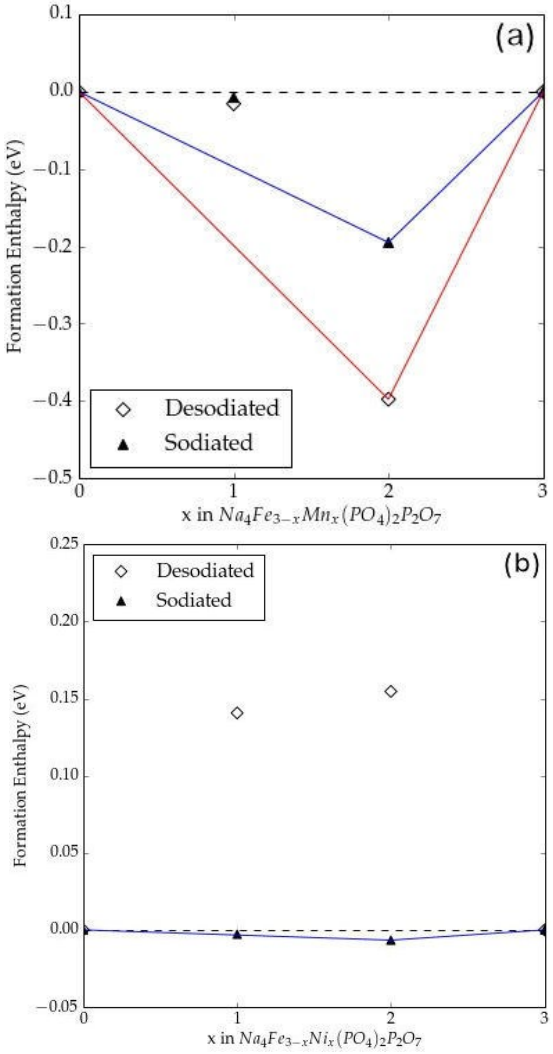


**Figure S2:** The energy of mixing per formula unit as a function of composition for Ni doping in $Na_4Fe_{3-x}M_x(PO_4)_2P_2O_7$ with (a) M=Mn and (b) M= Fe.

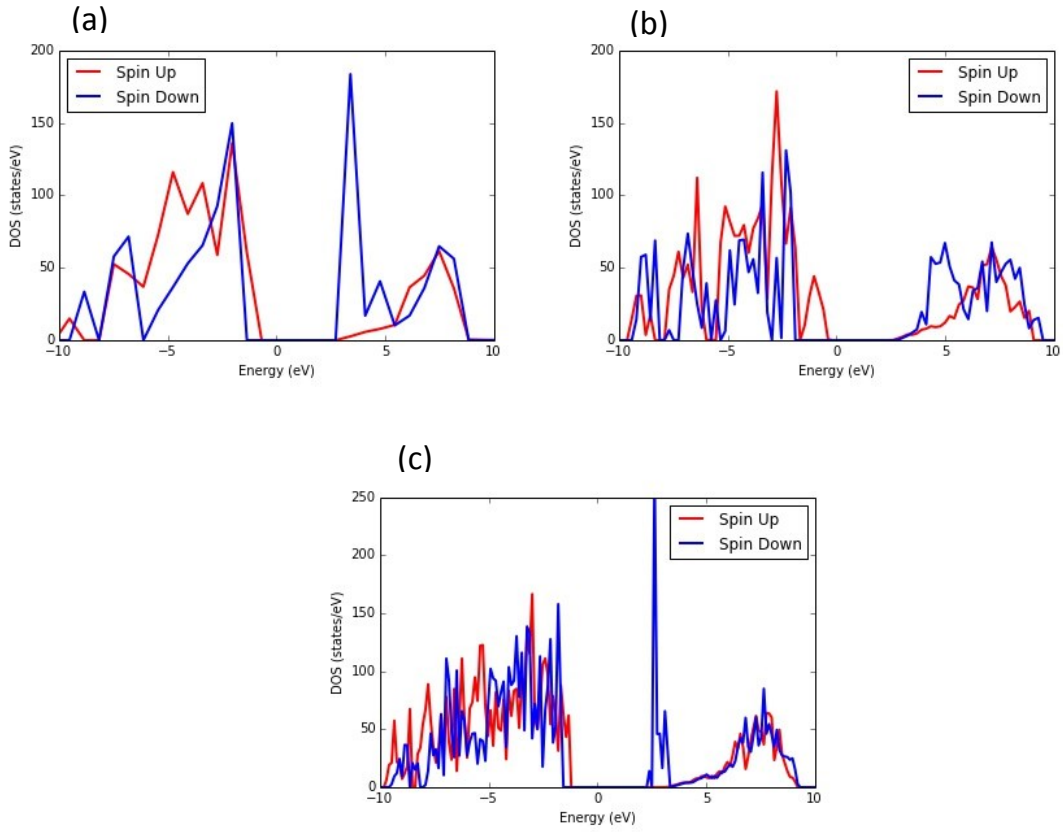


**Figure S3:** Density of states plots for $Na_4M_3(PO_4)_2P_2O_7$ with (a) M=Fe, (b) M=Mn and (c) M= Ni. The plots are centred with the Fermi level at 0 eV. All plots demonstrate a distinct band gap around the Fermi level.

**References for Supplementary Information**


1. Pedone A., Malavasi G., Menziani M. C., Cormack A. N. and Segre U., A New Self Consistent Empirical Interatomic Model for Oxides, Silicates and Silica-Based Glasses, *J. Phys. Chem. B*, **2006**, *110*, 11780-11795.

2. Kim H., Park I., Lee S., Kim H., Park K.-Y., Park Y.-U., Kim H., Kim J., Lim H.-D., Yoon W.-S., and Kang K., Understanding the Electrochemical Mechanism of the New Iron-Based Mixed-Phosphate $Na_4Fe_3(PO_4)_2P_2O_7$ in a Na Rechargeable Battery, *Chem. Mater.*, **2013**, *25*, 3614–3622.

3. Sanz F., Parada C., Rojo J. M. and Valero C. R., Synthesis, Structural Characterization, Magnetic Properties and Ionic Conductivity of $Na_4M_3(PO_4)_2P_2O_7$ (M = Mn, Co, Ni), *Chem. Mater.*, **2001**, *13*, 1334-1340.

4. Kim J. C., Moore C. J., Kang B., Hautier G., Jain A. and Ceder G., Synthesis and Electrochemical Properties of Monoclinic $LiMnBO_3$ as a Li Intercalation Material, *J. Electrochem Soc.*, **2011**, *158*, A309-A315.

5. Chen H., Hautier G., Jain A., Moore C., Kang B., Doe R., Wu L., Tang Y. and Ceder G., Carbonophosphates: A New Family of Cathode Materials for Li-ion Batteries Identified Computationally, *Chem. Mater.,* **2012**, *24*, 2009-2016.

6. Clark J. M., Eames C., Reynaud M., Rousse G., Chotard J. N., Tarascon J. M. and Islam M. S., High Voltage Sulphate Cathodes Li2M(SO4)2 (M = Fe, Mn, Co): Atomic-Scale Studies of Lithium Diffusion, Surfaces and Voltage Trends, *J. Mater. Chem. A*, **2014**, *2*, 7446–7453.

7. Ong S. P., Chevrier V. L., Hautier G., Jain A., Moore C., Kim S., Ma X. and Ceder G., Voltage, Stability and Diffusion Barrier Differences Between Sodium-Ion and Lithium-Ion Intercalation Materials, *Energy Environ. Sci.*, **2011**, *4*, 3680-3688.

8. Santamaria-Perez D., Amador U., Tartojada J., Dominiko R. and Arroyo-de Dompablo M. E., High Pressure Investigation of $Li_2MnSiO_4$ and $Li_2CoSiO_4$ Electrode Materials for Lithium-Ion Batteries, *Inorg. Chem.*, **2012**, *51(10)*, 5779-5786.

9. Saracibar A., van der Ven A. and Arroyo-de Dompablo M. E., Crystal Structure, Energetics and Electrochemistry of $Li_2FeSiO_4$ Polymorphs from First Principles Calculations, *Chem. Mater.*, **2012**, *24(3)*, 495-503.

10. Seo D.-H., Park Y.-U., Kim S.-W., Park I., Shakoor R. A. and Kang K., First Principles Study on Lithium Metal Borate Cathodes for Lithium Rechargeable Batteries, *Phys. Rev. B*, **2011**, *83*, 205127.

11. Kim S.-W., Seo D.-H., Kim H., Park K.-Y. and Kang K., A Comparative Study on $Na_2MnPO_4F$ and $Li_2MnPO_4F$ for Rechargeable Battery Cathodes, *Phys. Chem. Chem. Phys.*, **2012**, *14*, 3299-3303.

12. Seo D.-H,. Gwon H., Kim S.-W., Kim J. and Kang K., Multicomponent Olivine Cathode for Lithium Rechargeable Batteries: A First Principles Study, *Chem. Mater.*, **2010**, *22*, 518-523

13. Kim H., Seo D.-H., Kim H., Park I., Hong J., Park K.-Y. and Kang K., Multicomponent Effects on the Crystal Structures and Electrochemical Properties of Spinel Structured $M_3O_4$ (M = Fe, Mn, Co) Anodes in Lithium Rechargeable Batteries, *Chem. Mater.*, **2012**, *24(4)*, 720-725.

14. Kim H., Kim D. J., Seo D.-H., Yeom M. S., Kang K., Kim D. K. and Jung Y., Ab Initio Study of the Sodium Intercalation and Intermediate Phases in $Na_{0.44}MnO_2$ for Sodium-Ion Battery, *Chem. Mater.*, **2012**, *24(6)*, 1205-1211.

15. Lee D. H., Xu J. and Meng Y. S., An Advanced Cathode for Na-Ion Batteries with High Rate and Excellent Structural Stability, *Phys. Chem. Chem. Phys.,* **2013**, *15*, 3304-3312.

16. Qian D., Xu B., Chi M. and Meng Y. S., Uncovering the Roles of Oxygen Vacancies in Cation Migration in Lithium Excess Layered Oxides, *Phys. Chem. Chem. Phys.*, **2014**, *16*, 14665-14668.
17. Xu B., Fell C. R., Chi M. and Meng Y. S., Identifying Surface Structural Changes in Layered Li-Excess Nickel Manganese Oxides in High Voltage Lithium Ion Batteries: A Joint Experimental and Theoretical Study, *Energy Environ. Sci.*, **2011**, *4*, 2223-2233.
18. Fell C. R., Lee D. H., Meng Y. S., Gallardo-Amores J. M., Moran E. and Arroyo-de Dompablo M. E., High Pressure Driven Structural and Electrochemical Modifications in Layered Lithium Transition Metal Intercalation Oxides, *Energy Environ. Sci.*, **2012**, *5*, 6214-6224.
19. Yang M.-C., Xu B., Cheng J.-H., Pan C.-J., Hwang B.-J. and Meng Y. S., Electronic, Structural and Electrochemical Properties of $LiNi_xCu_yMn_{2-x-y}O_4$ ($0 < x < 0.5$, $0 < y < 0.5$) High-Voltage Spinel Materials, *Chem. Mater.*, **2011**, *23(11)*, 2832-2841.
20. Tompsett D. A., Parker S. C., Bruce P. G. and Islam M. S., Nanostructuring of B-$MnO_2$: The Important Role of Surface to Bulk Ion Migration, *Chem. Mater.*, **2013**, *25(4)*, 536-541.
21. Tompsett D. A. and Islam M. S., Electrochemistry of Hollandite a-$MnO_2$: Li-ion and Na-ion Insertion and $Li_2O$ Incorporation, *Chem. Mater.*, **2013**, *25(12)*, 2515-2526.
22. Seo D.-H., Kim H., Park I., Hong J. and Kang K., Polymorphism and Phase Transformations of $Li_{2-x}FeSiO_4$ ($0<x<2$) From First Principles, *Phys. Rev. B*, **2011**, *84*, 220106.
23. Eames C., Clark J. M., Rousse G., Tarascon J.-M. and Islam M. S., Lithium Migration Pathways and van der Waal Effects in the $LiFeSO_4OH$ Battery Material, *Chem. Mater.*, **2014**, *26*, 3672–3678.
24. Eames C., Armstrong A. R., Bruce P. G. and Islam M. S., Insights into Changes in Voltage and Structure of $Li_2FeSiO_4$ Polymorphs for Lithium-Ion Batteries, *Chem. Mater.*, **2012**, *24(11)*, 2155-2161.
25. Armand M., Tarascon J.-M. and Arroyo-de Dompablo M. E., Comparative Computational Investigation of N and F Substituted Polyoxoanionic Compounds: The Case of $Li_2FeSiO_4$ Electrode Material, *Electrochem. Commun.*, **2011**, *13(10)*, 1047-1050.
26. Armand M. and Arroyo-de Dompablo M. E., Benefits of N for O Substitution in Polyoxoanionic Electrode Materials: A First Principles Investigation of the Electrochemical Properties of $Li_2FeSiO_{4-y}N_y$ (y=0,0.5,1), *J. Mater. Chem.*, **2011**, *21*, 10026-10034.
27. Abdellahi A., Akyildiz O., Malik R., Thornton K. and Ceder G., Particle-Size and Morphology Dependence of the Preferred Interface Orientation $LiFePO_4$ Nano-Particles, *J. Mater. Chem. A*, **2014**, *2*, 15437-15447.
28. Vassilaras P., Toumar A. J. and Ceder G., Electrochemical Properties of $NaNi_{1/3}Co_{1/3}Fe_{1/3}O_2$ as a Cathode Material for Na-ion Batteries, *Electrochem. Commun.*, **2014**, *38*, 79-81.
29. Qian D., Hinuma Y., Chen H., Du L-S, Carroll K. J., Ceder G., Grey C. P. and Meng Y. S., Electronic Spin Transition in Nanosize Stoichiometric Lithium Cobalt Oxide, *J. Am. Chem. Soc.*, **2012**, *134(14)*, 6096-6099.
30. Jian Z. L., Hu H. J. and Zhou H. S., Designing High-Capacity Cathode Materials for Sodium Ion Batteries, *Electrochem. Commun.*, **2013**, *34*, 215-218.
31. Kim D. J., Ponraj R., Kannan A. G., Lee H. W., Fathi R., Ruffo R., Mari C. M. and Kim D. K., Diffusion Behaviour of Sodium Ions in $Na_{0.44}MnO_2$ in Aqueous and Non-aqueous Electrolytes, *J. Power Sources*, **2013**, *244*, 758-763.

32. Ruffo R., Fathi R., Kim D. J., Mari C. M. and Kim D. K., Impedance Analysis of $Na_{0.44}MnO_2$ Positive Electrode for Reversible Sodium Batteries in Organic Electrolyte, *Electrochim. Acta*, **2013**, *108*, 575-582.
33. Hung C. J., Lin P. and Tseng T. Y., Electrophoretic Fabrication and Pseudocapacitive Properties of Graphene/Manganese Oxide/Carbon Nanotube Nanocomposites, *J. Power Sources*, **2013**, *243*, 594-602.
34. Shibata T., Kobayashi W. and Moritomo Y., Sodium Ion Diffusion in Layered $Na_xCoO_2$, *Appl. Phys. Express*, **2013**, *6(9)*, 097101.
35. Shibata T., Kobayashi W. and Moritomo Y., Sodium Ion Diffusion in Layered $Na_xMnO_2$ ($0.49<x<0.75$): Comparison with $Na_xCoO_2$, *Appl. Phys. Express*, **2014**, *7(6)*, 067101.
36. Shu G. J. and Chou F. C., Sodium-Ion Diffusion and Ordering in Single Crystal P2-$Na_xCoO_2$, *Phys. Rev. B*, **2008**, *78(5)*, 052101.
37. Guo S. H., Yu H. J., Jian Z. L., Liu P., Zhu Y. B., Guo X. W., Chen M. W., Ishida M. and Zhou H. S., A High-Capacity, Low-Cost Layered Sodium Manganese Oxide Material as Cathode for Sodium-Ion Batteries, *ChemSusChem*, **2014**, *7(8)*, 2115-2119.
38. Deng C., Zhang S., Dong Z. and Shang Y., 1D Nanostructured Sodium Vanadium Oxide as a Novel Anode Material for Aqueous Sodium Ion Batteries, *Nano Energy*, **2014**, *4*, 49-55.
39. Bockenfield N. and Balducci A., Determination of Sodium Ion Diffusion Coefficients in Sodium Vanadium Phosphate, *J. Solid State Electrochem.*, **2014**, *18(4)*, 959-964.
40. Jiang T., Chen G., Li A., Wang C. Z. and Wei Y. J., Sol-gel Preparation and Electrochemical Properties of $Na_3V_2(PO_4)_2F_3$/C Composite Cathode Material for Lithium Ion Batteries, *J. Alloy Compd*, **2009**, *478*, 604-607.
41. Song W. X., Ji X. B., Wu Z. P., Yang Y., Zhou Z., Li F. Q., Chen Q. Y. and Banks C. E., Exploration of Ion Migration Mechanism and Diffusion Capability for $Na_3V_2(PO_4)_2F_3$ Cathode Utilized in Rechargeable Sodium-Ion Batteries, *J. Power Sources*, **2014**, *256*, 258-263.
42. Su L. Y., Winnick J. and Kohl P., Sodium Insertion into Vanadium Pentoxide in Methanesulfonyl Chloride-Aluminium Chloride Ionic Liquid, *J. Power Sources*, **2001**, *101(2)*, 226-230.
43. Vujkovic M. and Mentus S., Fast Sodiation/Desodiation Reactions of Electrochemically Delithiated Olivine LiFePO4 in Aerated Aqueous $NaNO_3$ Solution, *J. Power Sources*, **2014**, *247*, 184-188.
44. Wang Y. S., Yu X. Q., Xu S. Y., Bai J. M., Xiao R. J., Hu Y. S., Li H., Yang X. Q., Chen L. Q. and Huang X. J., A Zero-Strain Layered Metal Oxide as the Negative Electrode for Long-Life Sodium-Ion Batteries, *Nature Comm.*, **2013**, *4*, 2365.
45. Yu X. Q., Pan H. L., Wan W., Ma C., Bai J. M., Meng Q. P., Ehrlich S. N., Hu Y. S. and Yang X. Q., A Size-Dependant Sodium Storage Mechanism in Li4Ti5O12 Investigated by a Novel Characterization Technique Combining In-Situ X-ray Diffraction and Chemical Sodiation, *Nano Lett.*, **2013**, *13(10)*, 4721-4727.